DYNAMIC ANALYSIS OF SLOPE STABILITY DURING STRONG GROUND MOTION

by

K. TOKI and F. MIURA
Disaster Prevention Research Institute, Kyoto University

ABSTRACT

The stability of an existing slope during strong earthquake motion was investigated in detail by the nonlinear finite element technique. Joint elements were arranged at every interface between soil elements. Accordingly, each soil element is allowed to move in the directions parallel, perpendicular and rotationally to neighboring elements, namely, they can express a sort of sliding and separation at any interface between soil elements. As a preliminary analysis, static analyses were made and the results were compared with those obtained from the Janbu's method in order to check their compatibility.

Dynamic analyses were performed taking into account also the material nonlinearity. From the analyses performed it was found that the predominant period as well as the peak acceleration is significant in dynamic analysis while the safety factor is related only to the seismic coefficient in the static method.

INTRODUCTION

The influence of slope failure on daily life is greater each year, and a rational method to dynamically estimate the slope stability during earthquakes is of increasing importance. At present that most commonly used is the sliding circle method which is based on the seismic coefficient method. After the Izuhanto-oki earthquake in 1974 in which more than twenty peoples were killed by the slope failure, dynamic analyses were initiated using numerical methods. These, however, were limited to linear analyses.

In order to estimate the slope stability, a nonlinear analysis should be performed since the slope failure is a strongly nonlinear phenomenon which causes a great deal of residual displacement in soil and rock materials. The authors proposed a general method to analyze nonlinear dynamic soil structure interaction problems using the finite element method(1,2), in which the joint element(3) was employed to represent sliding and separation phenomena between the structure and soil. This proposed method is applied, in this paper, to investigate quantitatively the stability of an existing slope at the critical state in detail by examining soil material nonlinearity. Prior to dynamic analyses, static analyses are made by the nonlinear finite element technique and the results are compared with those obtained from the Janbu's method in order to check their compatibility.

STATIC ANALYSES OF SLOPE STABILITY BY THE FINITE ELEMENT METHOD

(1) The model analyzed

For an analysis of slope stability, the sliding circle, Bishop's and Janbu's methods are practically used, the choice of method depending on the shape of sliding surface(4). Although all are valid for static force, slope stability during dynamic forces can no longer be rationally estimated by these classical methods. The finite element method, however, makes it possible to estimate the dynamic stability of slopes during earthquakes, and the safety factor against sliding of the slope can, in particular, be directly estimated by adopting joint elements set along an arbitrary sliding surface.

Before any dynamic stability analysis is performed, static analyses are made by the finite element method and the results are compared with those obtained from classical methods in order to check their compatibility. Figure 1 is a cross section of an actual slope analyzed in this study. The slope is composed of banking and weathered rock under which lie slate basal rock, as determined by boring tests. The shear, V_S, and volumetric, V_P, wave velocities of each layer were obtained by the seismic prospecting. The material constants obtained by laboratory tests are listed in Table 1. However, the cohesion is parametrically changed to 0.02, 0.05 and 0.1 kg/cm^2 in the following analyses.

The finite element mesh of the model slope is shown in Figure 2. Joint elements are employed at every interface between the soil elements as shown schematically in Figure 3. All nodes are overlapped each other at initial state. Accordingly, each soil element is allowed to move in parallel, perpendicular and rotationally to the others, namely, they can express a sort of sliding and separation which occur in the actual situation. The solid, broken and irregular broken lines in Figure 2 designate sliding surfaces for which the safety factors have been calculated. These surfaces were decided with reference to those in a preliminary research.

(2) The results of static analyses

(a) A definition of safety factors in slope stability analyses

In order to estimate the stress state of the slope, the initial stresses due to the gravity force are first calculated and then, the stresses due to seismic force equivalent to the specified seismic coefficient are calculated under the initial stress states.

Slope stability is discussed based on two safety factors defined below when it is assessed by the finite element method.

(i) The local safety factor (LSF)

Sliding first occurs locally at some point in the slope and then propagates accompanied by stress redistribution. Let τ_y and τ be the yield and mobilized shear stresses of a joint element. The local safety factor is defined as the minimum value of the ratio $|\tau_y/\tau|$ of all joint elements.

(ii) The total safety factor (TSF)

The total safety factor indicates the safety against sliding of the entire area above the sliding surface under consideration. It is defined by:

$$TSF = \left| \sum_{j=1}^{N} \tau_{yj} l_j \Big/ \sum_{j=1}^{N} \tau_j l_j \right| \quad (1)$$

where, N is the number of joint elements forming the sliding surface and τ_{yj}, τ_j and l_j represent yield shear stress mobilized shear stress and the length of joint element j. In the case of dynamic analyses, the minimum values of the ratios with respect to the entire time analyzed are defined as LSF and TSF respectively.

(b) A comparison of the results obtained by Janbu's and the finite element methods

As Figure 2 shows, sliding surfaces are not circular arcs, and hence, the sliding circular method, based on the equilibrium of moment around the center of a sliding circle, can not be applied here. Janbu's method(4) is employed to estimate the safety factor, applicable to irregularly-shaped sliding surfaces. Sliding surfaces identical in shape and in element numbers were used to avoid differences in results due simply to differences in sliding surface shapes.

A comparison of safety factors in cases where cohesions, C_J=0.1 kg/cm^2 is made in Figure 4. Perfect agreement was obtained for Sliding surface 1, both monotonous and shortest. Sliding surfaces 2 and 3 which are longer and more complicated gave differences of 15∿20 % for the two methods used. One reason may be that inter-element stresses are not included in Janbu's method but are in the finite element method. An error may accumulate throughout the sliding surface and caused the differences in Figure 4. In general, however, the methods are in fairly close agreement.

(c) Slope stability for static force

TSFs are obtained for three sliding surfaces by changing the cohesion of the joint element C_J parametrically from 0.02 to 0.1 kg/cm^2. According to the results, the TSF of Sliding surface 1 is less than 1.0 at normal condition (k_H=0.0) and sliding will be caused by gravity force only when C_J=0.02 kg/cm^2. When C_J=0.05 kg/cm^2, Sliding surface 1 is in a critical state at normal conditions and will slide at k_H=0.1. The slope will slide if the cohesion is less than 0.05 kg/cm^2, even when there is no seismic force. Judging from the fact that the slope remains stable, the cohesion must be a non-zero value although it was zero in laboratory tests. Therefore, 0.1 kg/cm^2 is specified as the cohesion in the following analyses.

As the seismic coefficient increases, local sliding takes place and accompanies stress redistribution to the vicinity of the sliding surface after LSF=1.0, and when TSF=1.0 the sliding along the whole surface takes place. Figure 5 shows the TSFs and LSFs for three sliding surfaces. There is the possibility that Sliding surface 3 will slide locally even at normal conditions (Figure 5(c)). However, sliding along the entire surface does not take place because there is resistance of other elements of up to k_H=0.2. As for Sliding surface 1, the zone between LSF=1.0 and TSF=1.0 is so narrow that sliding of the whole sliding surface can easily take place once there is some local sliding. Thus, Sliding surface 1 is most likely to slide, followed by surface 3 and surface 2 is the most stable.

DYNAMIC ANALYSES OF SLOPE STABILITY BY THE FINITE ELEMENT METHOD

(1) Dynamic behavior of the slope during strong earthquake motion

Prior to seismic response analyses, eigenvalue analysis was performed and the fundamental natural frequency was 10.16 Hz. The slope was subjected to the simultaneous horizontal and vertical excitations of three different accelerograms, the El Centro NS and UD components (Imperial Valley Earthquake, 1940), the Jet Propulsion Laboratory (J.P.L.) S82E and UD components (San Fernando Earthquake, 1971) and the Hachinohe EW and UD components (1968 Tokachi-oki Earthquake, 1968). Table 2 lists the maximum amplitudes and predominant frequencies of the original accelerograms. The amplitude have been modified for use in seismic response analyses.

Figure 6 shows joint elements which slide and/or separate during the period of 2.0∿2.5 sec, or the main shock of the horizontal input acceleration, the NS component of the El Centro accelerogram. In this case (Case 1), acceleration amplitudes were not modified. In all joint elements sliding occurred along Sliding surface 1. Separation penetrated the slope from point A on the surface to point B at the base. Sliding was also observed along the interface between weathered and basal rock (the B-C line). Furthermore, most vertical joint elements show separation in the steep right-hand region of the slope, indicating the probability of collapse here. Sliding surfaces 2 and 3 are not sliding as a whole, although their sliding appears imminent.

Figure 7 shows joint elements sliding and/or separating when the slope has been subjected to the El Centro accelerograms whose amplitudes are reduced to 200 gal in the NS component and 117 gal in the UD component (Case 2). Not all of the joint elements are sliding and the stability is maintained along Sliding surface 1. When compared to Case 1, the number of joint elements which are sliding or separating in Case 2 are extremely reduced. The slope as a whole remains stable if the maximum horizontal input acceleration is less than 200 gal, although local sliding takes place and the slope begins sliding and the toe area collapses if the input acceleration exceeds the 200 gal level.

The maximum response distribution for Case 1 is shown in Figure 8 which shows horizontal acceleration. The response acceleration is amplified to more than 500 gal at the horizontal surface around the center of the slope. On the other hand, little amplification is observed in the right-hand region. The velocity distribution also is almost identical to acceleration. Maximum response values appear at or close to the area where geometrical change is remarkable.

(2) The influence of the predominant frequency of the excitation on slope stability

The slope was subjected to the J.P.L. (Case 3) and the Hachinohe (Case 4) accelerograms in addition to the El Centro accelerograms (Cases 1 and 2). Soil materials were assumed to be linearly elastic in these seismic response analyses. Time histories of the safety factor whose minimum value is the TSF are shown in Figure 9 for Sliding surface 1. Figure 9(a) is Case 1, (b) Case 2, (c) Case 3 and (d) Case 4. Sliding occurrences are denoted by the symbol ↓. It occurred five times

in Case 1 and twice in Case 4. In Case 1, sliding continued for a while in the first three occurrences but was instantaneous in the last two. In Case 4, sliding took place twice and continued for a while. The sliding magnitudes at the first three events in Case 1 and at the two events in Case 4 are greater than those at the last two events in Case 1 because sliding magnitude strongly depends on the sliding duration time. It is worth-while to note that the periods of input accelerograms on those occasions when sliding continued were relatively long. Sliding of the entire Sliding surface 1 did not take place in Cases 2 and 3 nor in any case of Sliding surfaces 2 and 3.

TSFs are summarized in Table 3 and they increased as the sliding surface changed, in all cases, in the order of Sliding surfaces 1, 3 and 2. This order coincides with that obtained from static analyses. TSFs were compared for each sliding surface. Case 1 had the lowest TSF and it increases in the order of Case 4, 2 and 3 for all sliding surfaces. The lowest TSF in Case 1 in all sliding surfaces is due to its having the largest input acceleration amplitude. The amplitude of horizontal acceleration in Cases 2, 3 and 4 are almost the same but the predominant frequencies differ. Therefore, TSF differences are caused by the differences in the predominant frequency of input accelerograms. The largest TSF are obtained in Case 3, which has the highest predominant frequency. The lowest TSFs were obtained in Case 4 with the lowest predominant frequency. The lower the predominant frequency, the more the slope is apt to slide, and slope stability strongly depends on predominant frequency. When slope stability is in question, attention, therefore, should be paid to the frequency content as well as to the input acceleration amplitude. In the static method, the safety factor is evaluated only by the maximum acceleration, or the seismic coefficient but in dynamic analyses, the predominant frequency of the acceleration as well as its maximum value is significant.

(3) The effects of the material nonlinearity of soil on slope stability

Material nonlinearity of soil was introduced here. The treatment of the nonlinearity is described in reference(2) in detail. The strength parameters such as the cohesion and angle of internal friction used here are listed in Table 1.

The shaded areas in Figures 10 and 11 show the elements which yielded during the time period of 2.0∿2.5 sec in Cases 1 and 2. A wide area has yielded in Case 1, but it is limited to the steep right-hand region in Case 2.

Figure 12 shows maximum response distribution of horizontal acceleration. The maximum response acceleration is about 450 gal and the area of 400 gal and over is limited to the surface surrounding the center of the slope. As the maximum value in the linear ground model was about 530 gal, soil nonlinearity reduced the maximum value by about 15 %. TSFs in Case 1 are tabulated in Table 4. Although Sliding surface 1 slides as a whole in both types of soil, TSFs in nonlinear soil are 10 % larger for Sliding surfaces 2 and 3. This implies that a lower TSF than there actually is is estimated when soil is assumed to be a linear elastic material.

When results here are compared to static analyses, the critical seismic coefficient k_H is 0.21 (206 gal) for Sliding surface 3. However, it does not slide but the TSF is greater than 1.0 (Table 4) even when as large an amplitude as 340 gal is applied. Sliding surface 1 is stable as shown in Figure 11 when the amplitude of excitation is 200 gal, although the critical seismic coefficient is 0.18 (176 gal). Lower TSFs than must actually exist are found by static methods and the difference can become 70 % as in the case of Sliding surface 3.

CONCLUSIONS

The stability of the present slope was quantitatively assessed for static and dynamic forces. From the analyses presented, the followings can be concluded:

(1) When safety against sliding was compared for Janbu's and the finite element methods, fairly good agreement was obtained, though in general the latter resulted in lower safety factors.

(2) Material nonlinearity of soil decreased response acceleration by 15 % and increased displacement. Higher safety factors of 5∿8 % were obtained when compared to the factors found when the slope was assumed to be linear elastic material.

(3) Although the critical seismic coefficient is 0.21 (206 gal) for the entire slope sliding (Sliding surface 3), it does not slide even when as large an amplitude as 340 gal is applied. For the local collapse (Sliding surface 1), it is stable when the excitation amplitude is 200 gal, although the critical seismic coefficient is 0.18 (176 gal).

(4) Safety factors strongly depends on the predominant frequency as well as the amplitude of the horizontal input accelerogram. The lower the predominant frequency, the lower the safety factor.

Although analytical examples have presented many useful information, there are still important problems to be solved or investigated.

This study was performed using the computer program 7S-II (Seismic Safety of Soil-Structure Systems considering Sliding and Separation, the second version). 7S-II will be provided on request by the authors.

ACKNOWLEDGEMENTS

The authors wish to express thier sincere gratitude to Mr. Yoshiyuki Oguni, former graduate student of Kyoto University, for his considerable assistance. Special appreciation is extended to Mr. Hideaki Kishimoto of Japan Computer Consultants, Osaka, for his advice regarding the programing of the computer codes.

REFERENCES

1) Toki k., T. Sato and F. Miura: Separation and sliding between soil and structure during strong ground motion, Int. J. Earthq. Engng Struc. Dyn., Vol.9, pp.263-277, 1981.
2) Toki K. and F. Miura: Nonlinear seismic response analysis of soil-structure interaction system, Int. J. Earthq. Engng Struc. Dyn. (in press).
3) Goodman R. E.: Methods of geological engineering in discontinuous rocks, West Publishing Company, Ch.8, pp.300-368, 1976.
4) Chowdhury R. N.: Slope analysis, Elsevier Scientific Publishing Company, Ch.1, 1978.

Table 1 Material constants and strength parameters of the slope

	Unit weight (tf/m^3)	Shear wave velocity (m/sec)	Poisson's ratio	Cohesion (kgf/m^2)	Angle of internal friction
Banking	1.6	150	0.4	0.1	29°
Weathered rock	1.9	300	0.4	0.1	45°
Joint element	Normal spring const. 3.0×10^5 tf/m^3 Shear spring const. 3.0×10^5 tf/m^3 ①Cohesion 0.1 kgf/cm^2 Friction angle 35° ②Cohesion 0.1 kgf/cm^2 Friction angle 25°				

Table 2 Maximum acceleration and predominant frequency of excitation accelerograms

	El Centro		J.P.L		Hachinohe	
	NS	UD	S82E	UD	EW	UD
Maximum acceleration (gal)	342	206	208	126	203	96
Predominant frequency (Hz)	1.15	8.55	2.88	2.95	0.83	1.25

Table 3 TSFs of the three sliding surfaces in the four cases

Case	Sliding surface 1	Sliding surface 2	Sliding surface 3
Case 1	Sliding (1.0)	1.150	1.057
Case 2	1.017	1.384	1.244
Case 3	1.125	1.508	1.308
Case 4	Sliding (1.0)	1.298	1.149

Table 4 The effects of soil nonlinearity on TSF

Case	Sliding surface 1	Sliding surface 2	Sliding surface 3
Linear Case (Case 1)	Sliding (1.0)	1.150	1.057
Non-linear Case	Sliding (1.0)	1.251	1.111

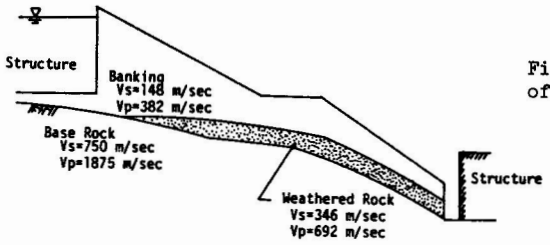

Fig.1 A cross section of the slope analyzed

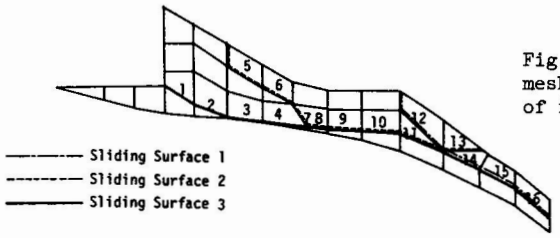

Fig.2 Finite element mesh of the model and of its sliding surfacce

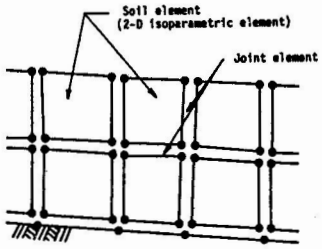

Fig.3 Discretization of the slope by solid and joint element

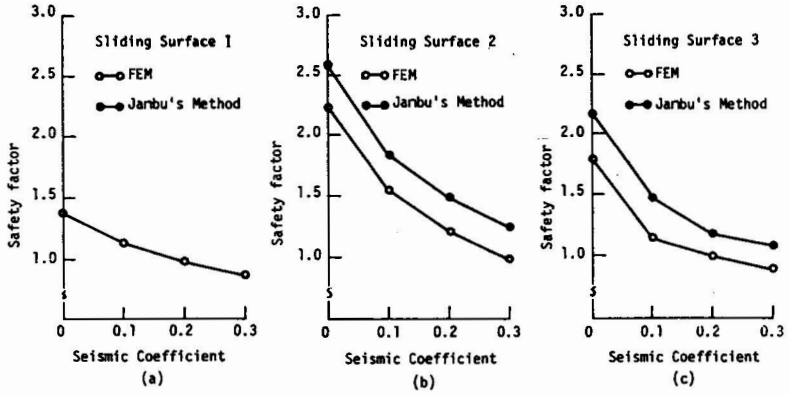

Fig.4 A comparison of safety factors from the seismic coefficient and proposed method

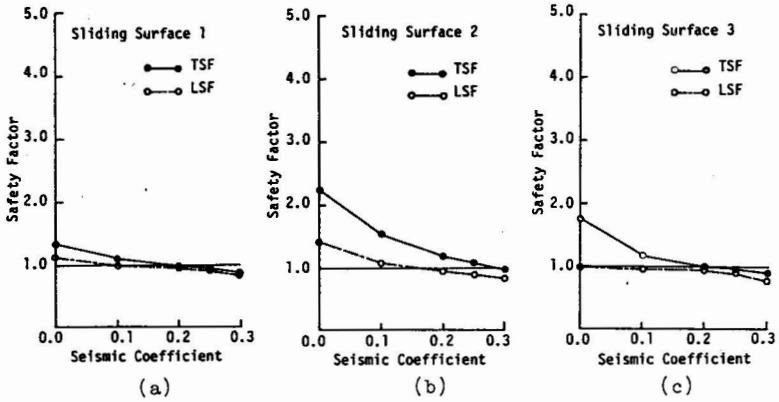

Fig.5 The relationship between TSF and LSF and the seismic coefficient (C_J = 0.1 kg/cm^2).

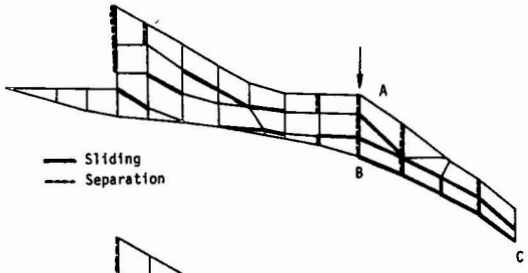

Fig.6 Joint elements showing sliding or separarion (El Centro 1940, 340 gal, t=2.0-2.5 sec)

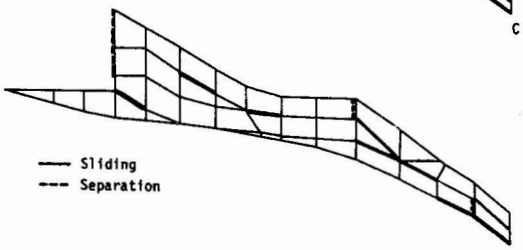

Fig.7 Joint elements showing sliding or separation (El Centro 1940, 200 gal, t=2.0-2.5 sec)

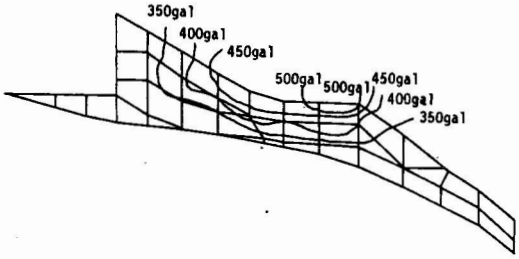

Fig.8 The distribution of maximum acceleration response

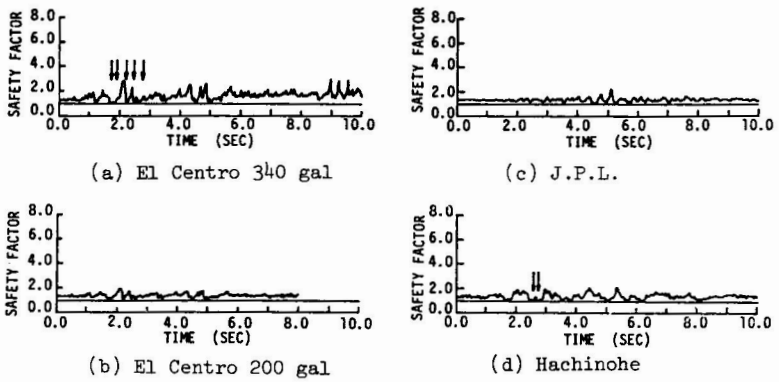

(a) El Centro 340 gal (c) J.P.L.

(b) El Centro 200 gal (d) Hachinohe

Fig.9 The relationship between TSF and input accelerograms

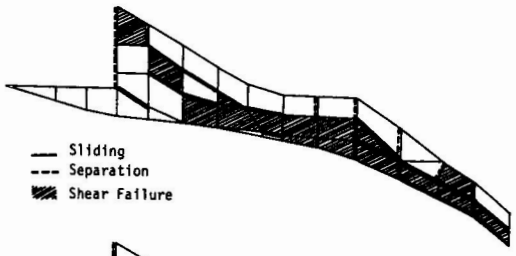

Fig.10 Shear failure zones and joint elements showing sliding or separation (El Centro 1940, 340 gal)

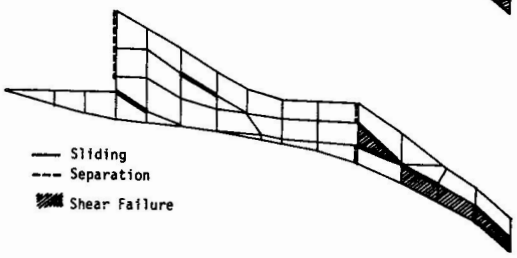

Fig.11 Shear failure zones and joint elements showing sliding or separation (El Centro 1940, 200 gal)

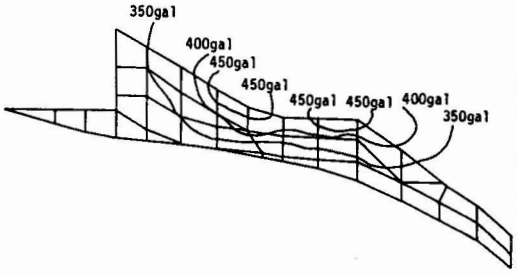

Fig.12 The distribution of maximum response acceleration when soil nonlinearity is taken into account (El Centro 1940, 340 gal)